Planetary Systems in the Universe: Observation, Formation and Evolution
ASP Conference Series, Vol. 3×10^8*, 2000*
A.J. Penny, P. Artymowicz, A.-M. Lagrange, and S.S. Russell, eds.

Ground interferometric searches

A. Glindemann, F. Delplancke, P. Kervella, F. Paresce, A. Richichi, M. Schöller

European Southern Observatory, 85748 Garching, Germany

Abstract. In this article, we discuss the instrumental requirements for planet searches from the ground. We review several methods and their fundamental limitations comparing the direct measurement of the visibility function (both modulus and phase) to astrometry and nulling interferometry. In particular, we will take the Very Large Telescope Interferometer (VLTI) as an example. The VLTI is an excellent facility for planet searches from the ground since it has both large apertures and long baselines, providing high SNR and milli arcsecond resolution.

1. Introduction

Since 1995, at least 50 objects classified as planets have been unambiguously detected (see compilation in http://www.obspm.fr/encycl/catalog.html) orbiting around nearby (10–20 pc) solar-like stars. Although there have been some doubts raised as to the reality of some of them, especially 51 Peg, subsequent even more refined observations have swept away all remaining doubts. As techniques get better, accuracy improves and surveys get more telescope time, this number is bound to increase dramatically.

Already, the statistics of the current searches indicates that planets are found around a few percent of the nearby solar-like stars. Since all of the discoveries so far, except Lalande 21185, have been made by means of the reflex velocity technique, the derived mass of the planet is always a lower limit and the true value will depend on the unknown inclination i of the orbit. This uncertainty disappears for the reflex motion technique used in precision astrometry as planned for the VLTI PRIMA facility.

2. The Very Large Telescope Interferometer

The Very Large Telescope (VLT) Observatory on Cerro Paranal (2635 m) in Northern Chile (see Fig. 1) reached a major milestone in September 2000 when the fourth of the 8-m Unit Telescopes saw first light. The preparation for first fringes of the VLT Interferometer (VLTI) has been advancing rapidly with the installation of two of the four Delay Line Systems in November 2000 (Glindemann et al. 2000). In the meantime, the 40-cm siderostats and all of the transfer optics have been installed and aligned, and the near infrared test instrument VINCI had first fringes with an artificial source in the VLTI beam combination laboratory at Paranal. First fringes with star light are planned for March 2001.

Early in 2002, two science instruments will be commissioned: MIDI, the mid infrared (N-band) two beam instrument, and AMBER, a near infrared (J, H, and K-band) three beam instrument. In 2003, PRIMA, the dual feed facility, will be installed to enable astrometric observations as well as imaging of faint sources with phase referenced observations. A collaboration with ESA is currently in preparation to install the ground demonstrator of the nulling interferometer satellite DARWIN in the VLTI beam combination laboratory.

The VLT Interferometer with its long baseline together with very large individual telescopes, with the choice amongst a large number of baselines, and with its wide scientific scope covering not only planet search but also stellar and extra galactic astronomy has the potential to establish interferometry as a key technique for modern astronomy.

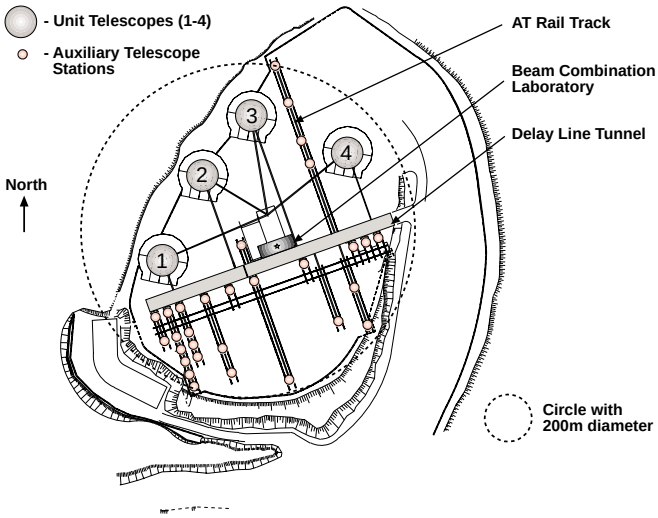

Figure 1. The layout of the VLTI. The four 8-m Unit Telescopes (UT) and the stations for the 1.8-m Auxiliary Telescopes (AT) are displayed. The AT stations are connected by rail tracks to relocate the ATs. Also shown are the Delay Line Tunnel and the beam combination laboratory. The Delay Line Tunnel has room for eight delay lines for the operation of eight ATs and a total of 28 baselines simultaneously. The longest baseline with two ATs is 200 m (indicated by the circle with 200 m diameter). The longest baseline with two UTs is 130 m.

3. Interferometry and planet detection

Interferometers with long baselines (e.g., up to 200 m with the VLTI) provide the angular resolution that is required to resolve close companions like those of 51 Peg and τ Boo. Long baselines are also the key to high precision astrometry since the error due to atmospheric turbulence scales with $B^{-2/3}$. Although the object geometry is rather simple (see Fig. 2) the extremely small brightness ratio $I_{rel} = 10^{-4}$–10^{-9} presents a serious problem because both the contrast of the

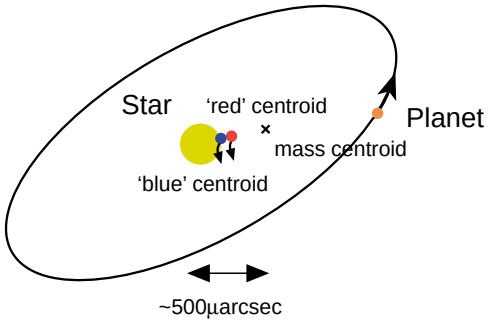

Figure 2. The geometry of a simple star/planet system: two point like objects orbiting around the centroid of the two masses. The 'light' centroid is much closer to the star than the mass centroid since the relative brightness of 10^{-4} to 10^{-9} of the planet is much smaller than its relative mass of about 10^{-3}. The position of the light centroid varies with wavelength. It should be noted that the light centroid moves closer to the star for larger separations whereas the mass centroid moves away from the star (see Sect. 4.2). The amplitude of the orbit is about 500 μarcsec for a Jupiter-Sun system seen from 10 pc.

fringe pattern and the phase of the visibility function scale with this number. Thus, phase or visibility measurements with an accuracy of I_{rel} are required to detect planets directly. The situation becomes more difficult if the separation d between star and planet increases since the relative brightness scales with $1/d^2$.

Since the star/planet system orbits around the mass centroid which is much further away from the star than the light centroid (see Fig. 2), astrometric observations can be used to measure the motion of the light centroid with respect to a reference source. This astrometric signature has an amplitude of 500 μarcsec for a Jupiter/Sun system seen from 10 pc, a typical distance for those planets that have been found so far. Therefore, the requirements for astrometry are more relaxed since the required accuracy of 50 μarcsec in the sky translates into an accuracy of typically 10^{-2} for the phase measurements. Astrometric detections are well suited for large planets and a large separation d since the astrometric signature increases linearly with d.

Nulling interferometry is an altogether different method for planet detection. It is a direct imaging technique rather than an interferometric method, the latter measuring fringe contrast and phase at different baselines. A nulling instrument produces a peculiar point spread function with a very deep (10^{-6}) and achromatic null on the optical axis allowing the direct observation of the - albeit unresolved - planet.

4. Direct Observations - Measurements of the visibility function

Both methods discussed in this section are particularly suited to detect small planets that are relatively close (a few milli arcsec, e.g. 1 AU at a few 100 pc) to the parent star and, thus, relatively bright. The closest star forming regions

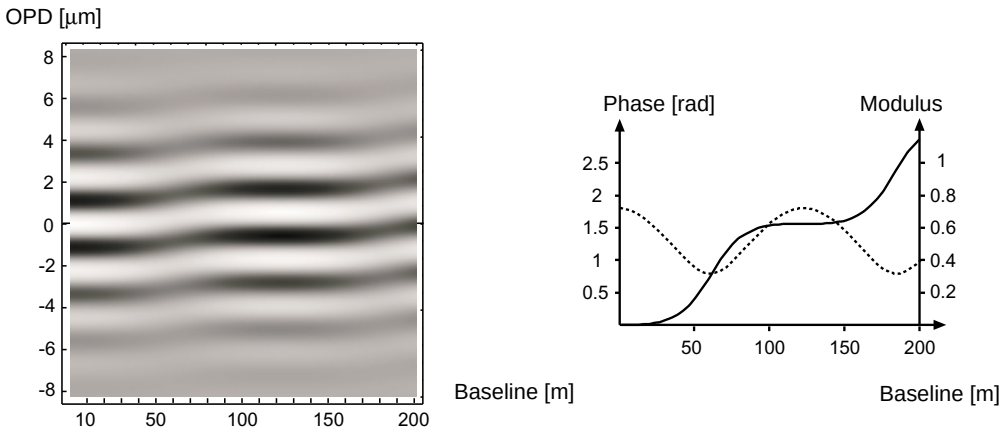

Figure 3. Simulated interferograms of τ Boo in the K-band for baselines between 0 and 200 m on the left, and the phase (solid line) and the modulus (dashed line) of the visibility function on the right. The baselines are set parallel to the star/planet axis. The vertical scans through the diagram on the left form the fringe pattern for each individual baseline. Due to the finite width of the wavelength band the contrast disappears for larger values of the optical path difference (OPD). The contrast of each fringe pattern is the modulus of the visibility for the particular baseline, and the displacement of the white light fringe is the phase displayed on the right. The relative luminosity of the companion of τ Boo is $3{\times}10^{-4}$ in the K-band and the phase would, thus, be 10^{-3} rad for a baseline of 200 m. Here, the relative brightness was arbitrarily set to 1/3 to make the fringe contrast visible.

(TW Hyd at ≈50 pc and Taurus Auriga at ≈140 pc) are within reach for these observations. For larger separations d the center of light moves closer to the planet, since the brightness of the planet goes down with $1/d^2$.

4.1. The modulus of the Visibility

The visibility varies in the uv-plane as a function of brightness ratio and planet position (see Fig. 3). Fig. 4 shows this for two epochs of a planet orbiting its parent star (Coudé du Foresto 1999). For the brightness ratio between star and planet of the order of 10^{-6}, the contrast variations in the visibility function over the visibility plane are also in the order of 10^{-6}, and thus difficult to detect.

The expected visibility accuracies for the VINCI test instrument in 5minute integrations are 5×10^{-2} without adaptive optics, 3×10^{-3} with adaptive optics but without fringe tracking, and $\ll 10^{-3}$ with fringe tracking.

These values are of course too low for a detection of the planet in one single 5 minute exposure. Synchronisation with radial velocity observations support this observing method by providing the period of the planet's orbit. Simulations by Coudé du Foresto (1999) have shown that with an observing time of 30 hours of the VLTI a SNR of 10 could be reached for τ Boo with the 1.8-m Auxiliary Telescopes.

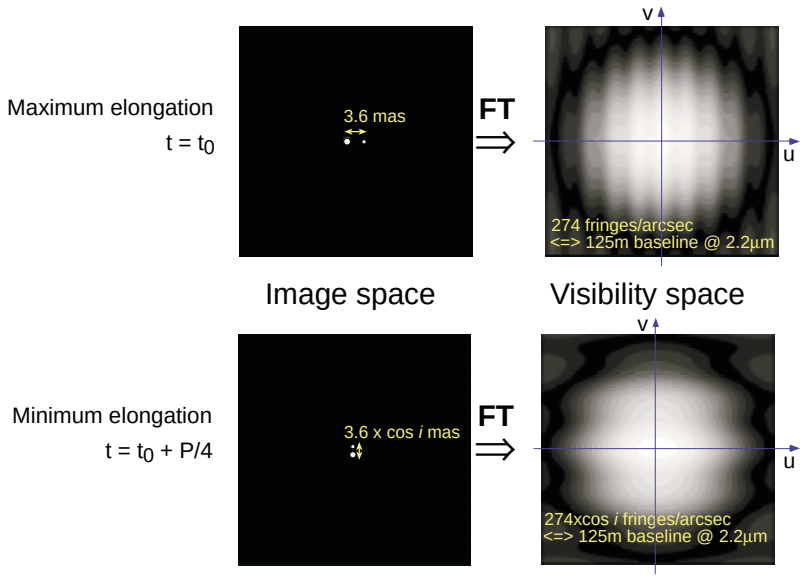

Figure 4. Object intensity distribution for two different epochs of the companion of 51 Peg on the left, and the corresponding visibility functions on the right. The fringes in the visibility function are orthogonal to the direction between star and planet. The spacing of the fringes is determined by the star/planet separation, the modulation of the fringes by the brightness ratio between the two objects. For demonstration purposes the brightness ratio has been set to 0.05 here. (Figures courtesy of V. Coudé du Foresto)

4.2. Differential Phase

Another technique to search for exoplanets makes use of the spectroscopic signature that the planet leaves in the phase of the complex visibility (Lopez, Petrov, & Vannier 2000) displayed in Fig. 5. Since the brightness ratio between star and planet becomes slightly more favorable for the planet at longer wavelengths, the apparent position of the star/planet system moves closer to the planet. This results in a change of the phase of the star planet system with wavelength. Since phase variations with wavelength can be introduced by the interferometer itself, special care has to be taken to calibrate the instrumental effects.

5. Indirect Detection - Astrometry

The accuracy of narrow-angle astrometry is eventually limited by atmospheric turbulence with an rms error of $\sigma_{\rm OPD} \propto B^{-2/3}\Delta S/\sqrt{t}$, with B the baseline, ΔS the distance of the two stars and t the observing time (Shao & Colavita 1992). For a 200 m baseline, a distance of 10 arcsec between the object and the reference star, and under typical atmospheric conditions at Paranal one can reach an accuracy of 10 μarcsec for a 30 minute integration.

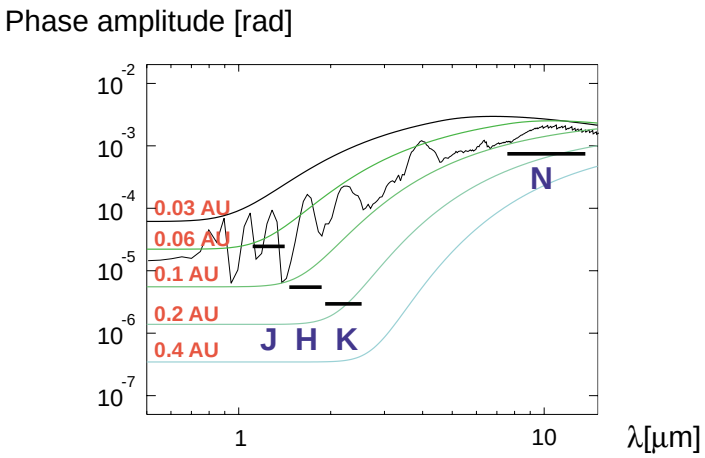

Figure 5. Phase amplitude vs. wavelength for various simulated planets. The straight lines are from blackbody 1.4 Jupiter-Mass planets around a Sun-like star at 10 pc, with semi major axis between 0.03 and 0.4 AU. Superimposed is a synthetic spectrum of 51 Peg b. The horizontal bars show the expected $1\,\sigma$ performance limits of AMBER (J, H, K) and MIDI (N) for 5 hours with UTs with a 80 m baseline and a spectral resolution of 25. (Figure courtesy of B. Lopez and R. Petrov)

This is sufficient to detect Jupiter/Sun systems at a distance of 10 pc with a reflex motion of ≈500 μarcsec. This measurement of the transverse reflex motion is analogue to the reflex velocity technique determining the longitudinal reflex motion. However, with astrometry the inclination angle i can be determined removing the ambiguity on the mass of the companion in the $M \sin i$ product.

In Fig. 6 this technique is illustrated. The technical challenge lies in the precise (5 nm accuracy over 30 minutes) measurement of the internal optical path difference ($\mathrm{OPD_{int}}$). A dedicated laser metrology will be used in PRIMA, the dual feed facility of the VLTI to perform this task (Quirrenbach et al. 1998, Delplancke et al. 2000). The OPD due to atmospheric turbulence ($\mathrm{OPD_{turb}}$) is averaged out, and the phase ϕ of the visibility function is negligible for a star/planet system (see Sect. 3). Measuring also the baseline B with a precision of 50 μm, an accuracy of 10 μarcsec can be reached for the astrometric signature.

6. Nulling Interferometry

The concept of nulling interferometry for planet detection was originally proposed by Bracewell & MacPhie (1978). The finite bandwidth of interferometric observations limits the OPD range where fringes can be found and it diminishes the contrast for increasing OPD (see e.g., the low contrast for OPD = $\pm 8\,\mu$m in Fig. 3). The dark fringes are not perfectly dark since their position – given by OPD = $\lambda/2$ – varies over the band. The white light fringe of a neighboring planet would still be fainter than the dark fringe of the star. However, producing

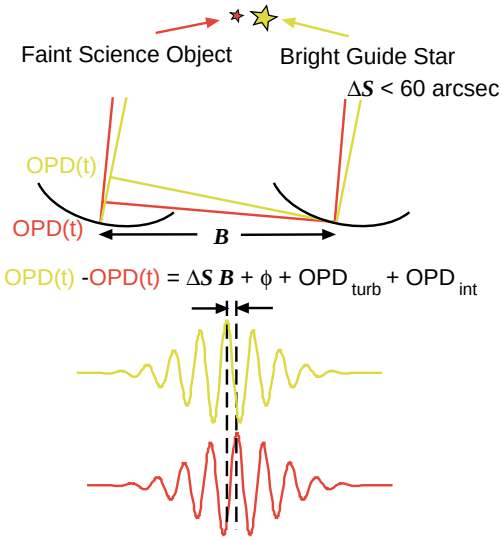

Figure 6. Principle of narrow angle astrometry. The difference in the positions of the white light fringes of object and reference star are determined by the OPD given by the product of ΔS – the angular separation vector of the stars – and B – the baseline vector – by the phase ϕ of the visibility funtion of the science object, by the OPD caused by the turbulence, and by the internal OPD.

an achromatic dark fringe at zero OPD, one could detect objects down to a level given by straylight and residual aberrations in the wavefront. Nulls as low as 10^{-4} have been achieved experimentally by Serabyn (1999). By arranging the individual telescopes, the point spread function is shaped tuning the interferometer to detect planets with a separation from the star that is determined by the distance between the null and the first sidelobe.

It should be noted that rather than measuring the contrast of the fringe pattern, a direct imaging technique is applied here. Usually, the point spread function in Fig. 7 is called the transmission map which is a different way of looking at this technique but leading to the same result.

The advantage of nulling interferometry over the other methods discussed so far is that a wide wavelength band can be used, increasing the sensitivity. This is of particular importance in space where the wavelength range is not restricted by atmospheric bands. From the ground, the influence of the residual aberrations on the depth of the null is rather serious since a very high order adaptive optics system is required to correct the wavefront.

7. Conclusions

The performance of ground based interferometers like VLTI is sufficient to discover giant planets with astrometry, and to detect and obtain infrared spectra

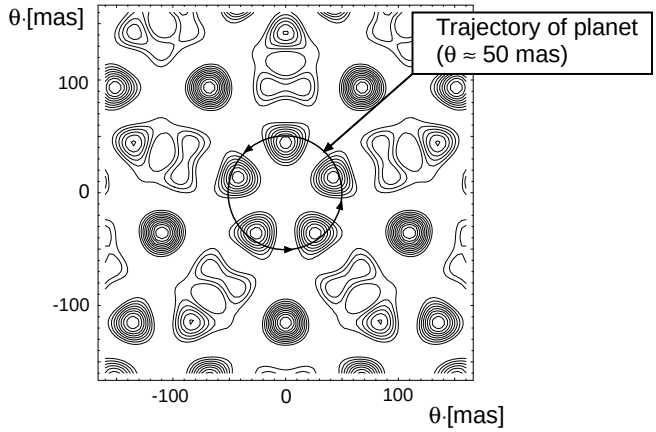

Figure 7. Point spread function of the nulling interferometer array proposed by Mennesson & Mariotti (1997). The five telescopes are arranged on a circle with a diameter of 50 m. At a wavelength of 10 μm the first sidelobes are at a distance of ≈50 mas.

of hot Jupiters. Searching for exoplanets is time consuming but it can also be done with the 1.8-m Auxiliary Telescopes. Ground based observations form a stepping stone both technically and scientifically for future space programmes.

References

Bracewell, R.N. & MacPhie, R.H. 1978, Nature, 274, 780

Coudé de Foresto, V. 1999 in Proc. of the ESO Symposium, From Extrasolar Planets to Cosmology: The VLT Opening Symposium, ed. J. Bergeron & A. Renzini (Berlin, Heidelberg, New York: Springer), 560

Delplancke, F., Leveque, S., Kervella, P., Glindemann, A., & d'Arcio, L. 2000 in Interferometry in Optical Astronomy, SPIE Vol. 4006, 365

Glindemann, A., Abuter, R., Carbognani, F., Delplancke, F., Derie, F., Gennai, A., Gitton, Ph., Kervella, P., Koehler, B., Lévêque, S., Menardi, S., Michel, A., Paresce, F., Phan Duc, T., Richichi, A., Schöller, M., Tarenghi, M., Wallander A., & Wilhelm, R. 2000 in Interferometry in Optical Astronomy, SPIE Vol. 4006, 2

Lopez, B., Petrov, R.G., & Vannier, M. 2000 in Interferometry in Optical Astronomy, SPIE Vol. 4006, 407

Mennesson, B. & Mariotti, J.-M. 1997, Icarus, 128, 202

Quirrenbach, A., Coudé de Foresto, V., Daigne, G., Hofmann, K.-H., Hofmann, R., Lattanzi, M., Osterbart, R., le Poole, R., Queloz, D., & Vakili, F. 1998 in Astronomical Interferometry, SPIE Vol. 3350, 807

Serabyn, E. 1999, Appl. Opt., 28, 4213

Shao, M. & Colavita, M.M. 1992, A&A, 262, 353